forests

MDPI

Article

ALS-Based, Automated, Single-Tree 3D Reconstruction and Parameter Extraction Modeling

Hong Wang [1], Dan Li [1,*], Jiaqi Duan [1] and Peng Sun [2]

[1] Forestry Information Engineering Laboratory, Northeast Forestry University, Harbin 150040, China; wanghong5424@126.com (H.W.); duanjiaqi0124@126.com (J.D.)
[2] College of Information and Computer Engineering, Northeast Forestry University, Harbin 150040, China; masyam12@126.com
* Correspondence: ld725725@126.com

Abstract: The 3D reconstruction of point cloud trees and the acquisition of stand factors are key to supporting forestry regulation and urban planning. However, the two are usually independent modules in existing studies. In this work, we extended the AdTree method for 3D modeling of trees by adding a quantitative analysis capability to acquire stand factors. We used unmanned aircraft LiDAR (ALS) data as the raw data for this study. After denoising the data and segmenting the single trees, we obtained the single-tree samples needed for this study and produced our own single-tree sample dataset. The scanned tree point cloud was reconstructed in three dimensions in terms of geometry and topology, and important stand parameters in forestry were extracted. This improvement in the quantification of model parameters significantly improves the utility of the original point cloud tree reconstruction algorithm and increases its ability for quantitative analysis. The tree parameters obtained by this improved model were validated on 82 camphor pine trees sampled from the Northeast Forestry University forest. In a controlled experiment with the same field-measured parameters, the root mean square errors (RMSEs) and coefficients of determination (R^2s) for diameters at breast height (DBHs) and crown widths (CWs) were 4.1 cm and 0.63, and 0.61 m and 0.74, and the RMSEs and coefficients of determination (R^2s) for heights at tree height (THs) and crown base heights (CBHs) were 0.55 m and 0.85, and 1.02 m and 0.88, respectively. The overall effect of the canopy volume extracted based on the alpha shape is closest to the original point cloud and best estimated when alpha = 0.3.

Keywords: AdTree; tree modeling; tree parameter extraction

Citation: Wang, H.; Li, D.; Duan, J.; Sun, P. ALS-Based, Automated, Single-Tree 3D Reconstruction and Parameter Extraction Modeling. *Forests* **2024**, *15*, 1776. https://doi.org/10.3390/f15101776

Academic Editors: Marcos Benedito Schimalski, Vasco M. Mantas and Camile Sothe

Received: 6 September 2024
Revised: 24 September 2024
Accepted: 2 October 2024
Published: 9 October 2024

1. Introduction

Tree stand factor measurement and tree modeling are two popular research directions in digital forestry research today. Stumpage factor extraction is the basis for assessing the growth status of forest trees in sample plots as well as evaluating important attributes such as forest stumpage, biomass, and carbon stock, which are of great significance for forestry resource management [1]. The accurate acquisition of stumpage parameters plays a decisive role in understanding the structure and function of forests, predicting forest growth and productivity, assessing forest health, and developing effective forest management and conservation strategies [2]. Methods for obtaining stumpage factors include traditional field-based surveys and modern remote surveys [3]. Traditional field-based surveys usually require manual measurement with traditional measuring tools, which involves destructive sampling, has a low degree of automation, and requires specialized personnel to operate [4]. The non-contact method utilizes modern technological equipment, such as laser scanners [5,6], cameras [3], drones [7], and remote sensing technology [8,9], to obtain tree stand parameters from a remote location. This method not only avoids damage to the sampling site but also improves the accuracy and efficiency of measurement, while

the non-contact measurement method can also be used to continuously monitor the forest, providing a more scientific, dynamic, data-oriented basis for forest protection.

The three-dimensional modeling of trees has numerous applications across a variety of fields, such as urban landscape design, ecological simulation, forestry management, and ecological research, as outlined by Kurdi F.T. et al. [10]. Accurate tree modeling not only improves the realism of the landscape but also represents a promising approach for the scientific management of vegetation and implementation of precision forestry [11]. Conventional tree modeling includes the rule-based modeling approach for trees using recursive branching, first proposed by Honda [12], and subsequent sketch-based [13], image-based [14], and LiDAR-based [15] modeling, proposed by Okabe et al. LiDAR-based modeling schemes have the advantage of higher data accuracy over other models [16].

To address the challenge of integrating high-precision, automated tree modeling with non-destructive parameter acquisition, recent advancements in LiDAR technology have significantly transformed the methods used in forestry. LiDAR has the ability to detect the spatial structural characteristics of forest vegetation, especially the forest's vertical structural parameters due to its high sampling intensity and strong vegetation penetration, and has greater advantages than previous optical remote sensing equipment [17]. González-Jorge et al. [18] and Petrie et al. [19] confirmed that the point cloud data acquired with laser scanners have very high density and quality, with speeds typically reaching 100 kHz to 1 MHz or even higher, and up to sub-centimeter accuracy. Several types of laser scanning systems exist, and the three main categories distinguished by application area are terrestrial LiDAR [20], satellite-borne LiDAR [21], and airborne LiDAR [22]. According to Holopainen et al. [23], it is difficult to obtain high-precision canopy information with ground-based LiDAR during the data scanning process. In addition, satellite-borne LiDAR has a long data acquisition cycle and low data accuracy due to the relatively long measurement distance, making it only applicable to large-scale and long-cycle forestry surveys, as detailed by Sun et al. [24]. In view of the reasons mentioned above, we used unmanned aircraft LiDAR (ALS)-scanned point cloud data as this study's initial data.

Despite the advancements made by existing quantitative tree structure models such as TreeQSM [25] and AdQSM [26], these models still exhibit notable limitations. TreeQSM, developed by Pasi Raumonen et al. [25], has been widely adopted for tree modeling and validated through destructive experiments, demonstrating high accuracy in parameter extraction. However, it has limitations in reconstructing tree models with reasonable geometric topology, particularly in branching structures. Although AdQSM [26] offers improvements over TreeQSM in certain modeling aspects, it performs poorly in branch parameter analysis. Given the scarcity and limitations of existing tree quantification models, there is a need to develop more precise models, particularly those based on ALS (Airborne LiDAR Scanning) point clouds, for estimating tree attributes. This study addresses these gaps by proposing an ALS-based automatic, single-tree 3D reconstruction and parameter extraction model. The proposed method integrates high-precision, automated, and non-destructive tree parameter acquisition, improving both the accuracy and efficiency of tree modeling. We will further elaborate on these limitations and provide a comparative analysis with existing studies in the Results Section.

The main methods in the early studies of LiDAR-based trunk parameter acquisition were least squares circle fitting (Calders K. et al. [27]), Hough transform circle detection (Trochta J. et al. [28]), RANSAC circle detection (Zhou S. et al. [29] and Olofsson et al. [30]), cylindrical fitting (Yang B. et al. [31]), and so on. Projecting the point cloud's horizontal layer onto the plane for two-dimensional curve fitting is a common technique for extracting breast diameter [27]. However, this method has two main issues: it involves all point clouds during circle fitting, making it unsuitable for noisy data, and it suffers from accuracy loss due to the axial and radial directions of the horizontal layers not being calculated together. Robust methods like two-dimensional Hough transform, RANSAC, and minimum median can mitigate noise effects but may mistakenly identify non-trunk point clouds as tree trunks. To address the issue of precision loss in the conversion from three-dimensional to

two-dimensional data, the use of cylindrical fitting methods proves to be more effective [32]. In terms of canopy parameter extraction, canopy volume is one of the most difficult tree parameters to obtain, according to Dai M. et al. [33]. Early approaches approximated tree shapes with simple geometries and used empirical formulas [34]. However, selecting an appropriate shape is somewhat subjective and usually applies to common urban tree species [35]. However, in reality, tree crown shapes are generally irregular [36], so this is a rough metric. Subsequently, the convex packet algorithm, voxel simulation, and alpha-shape triangular mesh construction were proposed. As early as 1995, Cluzeau et al. [37] explored the application of the 3D convex packet algorithm to the computational derivation of crown volume. Since the convex packet method is considered simple and general, numerous research studies have employed it to generate crown parameters by simulating crown volume [38]. But this method produces a larger error for trees with large cavity volumes [39]. In 2005, Phattaralerphong and Sinoquet [40] proposed voxelization for crown volume computation, but this method's results are highly dependent on voxel size and can generate numerous empty voxels for complex shapes [41]. In 2008, Zhu et al. [42] proposed the application of the alpha-shape algorithm to reconstruct the shape of scanned crowns and achieved better reconstruction results. The method was subsequently applied to crown volume estimation [43]. The alpha-shape algorithm determines the boundary based on the alpha value, and as alpha increases towards infinity, the alpha shape approaches a convex hull at a given point (the convex hull section). As alpha decreases, the shape shrinks and gradually forms a cavity. Although the boundary shape is directly affected by the parameters, as in the voxel method, the alpha parameter in the alpha-shape algorithm provides the ability to adjust the fineness of the shape, allowing the user to employ trade-offs between capturing details and removing noise, as needed.

In 2019, Shenglan Du et al. [11] proposed an automatic, detailed, and accurate tree modeling method based on laser scanning. The AdTree method showed strong robustness in modeling trees of different types and sizes, and the overall fitting error was less than 10 cm. Although the AdTree method significantly advanced the field of tree modeling, there are still some limitations in its modeling approach, especially when it cannot be quantified. This study aims to address these limitations by extending the functionality of the AdTree method as outlined by Shenglan Du et al. [11]. Specifically, we have introduced additional algorithms, including branch-trunk cylindrical fitting, Welzl's minimum outer circle, and crown alpha-shape triangular mesh construction. These algorithms enable us to extract key parameters such as tree height (TH), crown base height (CBH), diameter at breast height (DBH), crown width (CW), and crown volume (CV) with greater precision. Our method aims to assess the accuracy and feasibility of models with parameter quantification and the three-dimensional reconstruction capabilities in specific forestry research scenarios. To validate the effectiveness of our approach, we constructed a dedicated dataset and conducted field measurements on 82 trees within the sample area. By comparing and analyzing these field measurements, we confirmed the feasibility and validity of our method, achieving the specific objectives of this study.

2. Materials and Methods

2.1. Study Area

As shown in Figure 1, the study area is an urban forestry demonstration base of Northeast Forestry University, which is located at the junction of the Nangang and Xiangfang districts in Harbin City, Heilongjiang Province, China, adjacent to Majiagou, which is an important forestry research and practice base in Northeast China. The geographic coordinates of this experimental base are 45°43′10″ N, 126°37′15″ E, with an elevation of 136–148 m and a total area of about 43.95 ha, as indicated by the red line in Figure 1. It has a typical temperate, continental monsoon climate. The average annual temperature is 3.5 °C, and the average annual precipitation is about 570 mm. The terrain of the study area is flat, and the soil type is zonal black calcareous soil with good moisture conditions. The tree species of this study is the camphor pine, which is an evergreen coniferous tree commonly

found in Asia and widely planted in streets and parks in Northern China, covering a total area of approximately 0.56 ha, as indicated by the blue line in Figure 1.

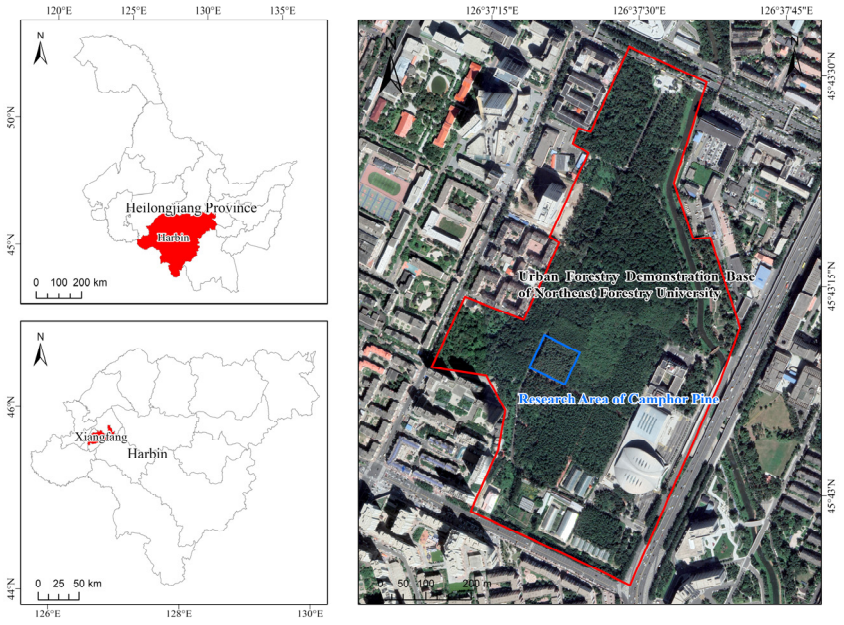

Figure 1. Overview map of the study area.

2.2. ALS Data

2.2.1. ALS Data Acquisition Program

The data acquisition equipment was a DJI UAV Warp M300 RTK equipped with a DJI Zenmuse L1 LiDAR device (SZ DJI Technology Co., Ltd., Shenzhen, China). The scanning was conducted on 26 October 2022, and took about 30 min. One 80 m × 75 m study area was laid out within the flight coverage of the UAV, with distinct markers for the area boundaries, and all trees were numbered sequentially. A total of 148 camphor pines were planted in the collection area in the evergreen foliage state. The altitude of the flight path was set to 40 m, and the flight speed was 3 m/s. In order to maximize the efficiency of data collection, the "S-shaped" route was adopted, and the repeated scanning mode was used to ensure the completeness of data collection. Regarding the flight parameters, the heading overlap rate was 70%, the side overlap rate was 65%, the sampling rate was 160 kHz, and the triple echo type was adopted. Based on the above scheme, we obtained the raw data, including laser, RTK, and camera calibration data. We successfully converted the LiDAR data into standard .LAS or .PLY format files by using the DJI Terra_4.0.1 software for processing.

2.2.2. ALS Data Preprocessing

The data preprocessing steps mainly include denoising, ground filtering, and individual tree segmentation. In the denoising and ground filtering stages, we mainly utilized the open-source software CloudCompare_2.13.alpha for processing, the effect of which is shown in Figure 2a–c. During the scanning process, the point cloud data may be affected by noise due to the presence of external disturbances such as light, haze, equipment vibration, and diffuse reflection on the object's surface. In order to deal with this noise, the statistical filtering algorithm was chosen in this study for the denoising operation. Specifically, we set the number of proximity points parameter to 50 and the standard deviation multiplier to 1.0. After the filtering process, the total number of points in the dataset was reduced from the initial 8,058,806 to 7,239,092, indicating that the filtering algorithm effectively removes the noise and retains the main data features. The result of this denoising operation shows a better effect and a clearer and more reliable database for the subsequent processing and analysis of point cloud mono-wood segmentation data. The initial point cloud data collected by ALS contain bare surface point clouds. Accordingly, in order to filter the surface

information and separate ground features, the CSF (Cloth Simulation Filter) fabric filtering algorithm [44] is utilized to separate the ground points. Based on the comprehensive consideration of the features of the ground features and the filtering effect, in CloudCompare, the fabric grid size was set to 0.5, the maximum number of iterations was set to 500, and the threshold was set to 0.6. Figure 2c shows the effect after the ground features were separated. The random walker segmentation algorithm proposed by Shendryk et al. was used for mono-wood segmentation in this study [45]. This was achieved in the Linux environment in combination with the PCL library and C++. Unlike most of the top-down, point cloud, single-tree depiction algorithms, this method is a lightweight, bottom-up, individual tree segmentation method from trunk to crown, which also has high segmentation accuracy for trees with complex shapes [24]. A total of 148 camphor pine trees were processed in the experiment, and the final segmentation results are shown in Figure 2d. We screened the segmented individual tree point clouds one by one, manually deleted the tree point cloud data with high incompleteness and overlap (refer to Figure 3), and selected 82 samples with more complete data after segmentation as the experimental samples.

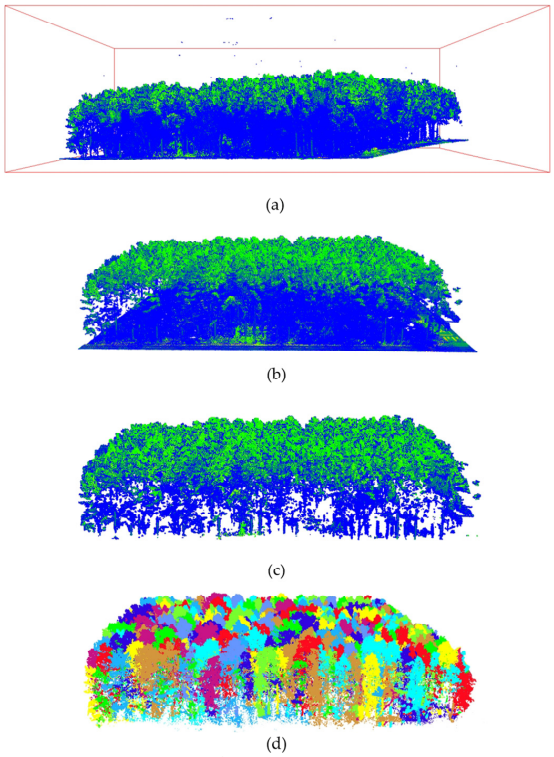

Figure 2. (**a**) Side view of the original point clouds with noise. (**b**) Point clouds after denoising. (**c**) Point clouds with ground points removed. (**d**) The results of the segmentation algorithm. The colors of the point clouds in subfigures (**a**–**c**) are the "Scalar field" pattern in CloudCompare.

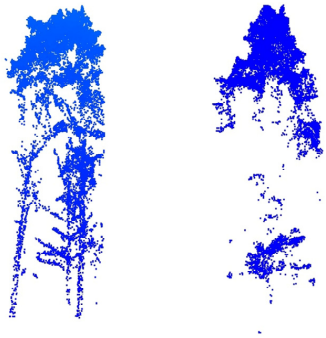

Figure 3. Overlapping point cloud trees and point cloud trees with low completeness.

2.3. Field Measurements in the Field

Our field data collection was conducted on 27 October 2022, involving three participants over a total duration of three days. The field measurement results are shown in Table 1. During data collection, we laid out a sample plot of 80 m × 75 m within the UAV flight coverage. The four corners of the sample plot were labeled as points A, B, C, and D, and obvious markers were set to indicate the boundaries so as to facilitate the accurate positioning of the ALS data collection and to ensure the consistency and accuracy of the measurement range. All trees within the sample plot were numbered sequentially and manual measurements were taken to record RTK positioning, tree height, crown base height, diameter at breast height, and crown width according to the following measurement methods:

- Tree height (TH) is the distance from the rootstock of the tree at ground level to the highest point of the canopy, usually measured by triangulation using a Blume–Leiss altimeter (Nanjing Xiangruide Electrical Technology Co., Ltd., Nanjing, China). When an altimeter is used to measure the height of an unknown point, the sight hole forms a straight line with the apex of the tree. The angle between the straight line and the horizontal line is θ. The horizontal distance from the person to the tree L and the height of the person h are known, and the height of the tree can be obtained from the tangent function as $H = L \times \tan\theta + h$.
- Crown base height (CBH) refers to the height of the tree ground at the rootstock to the bottom of the crown. The measurement method refers to the triangulation method of tree height in which the Blume–Leiss altimeter sighting hole is aimed at the bottom of the crown.
- Diameter at breast height (DBH) refers to the cross-sectional diameter of the tree trunk at breast height. This value can be obtained by measuring the circumference of the trunk at breast height with a tape measure (C), then $DBH = C/\pi$.
- Crown width (CW) usually refers to the average value of the crown width in the north–south direction and the width in the east–west direction. Given that the horizontal projection distance in the north–south direction is NS, and the horizontal projection distance in the east–west direction is EW, the crown width $CW = (EW + NS)/2$.

Table 1. Field measurement results.

	Average Value	Maximum Value	Minimum Value
TH (m)	17.95	20.73	13.82
CBH (m)	7.02	13.89	3.35
DBH (cm)	30.8	47.1	14.4
CW (m)	5.32	8.87	3.10

2.4. AdTree-Based 3D Model Reconstruction of Trees

For tree model reconstruction, we adopted the AdTree method proposed by Shenglan Du et al. [11]. In the reconstruction process, AdTree is used to construct the initial tree skeleton based on the intrinsic spatial distribution of the input points. On the one hand, the Minimum Spanning Tree (MST) algorithm was utilized to efficiently extract the initial skeleton of the tree from the input point cloud. On the other hand, specific skeleton optimization strategies were developed to maintain the natural and realistic topology of the tree branches.

The AdTree method is remarkably adaptive and robust in handling the 3D reconstruction of diverse tree species and trees of different sizes. The method can be used to effectively reconstruct highly accurate tree models from point cloud data with a clear branching structure. AdTree can more realistically reproduce the details of tree trunks and branches compared with other open-source tree modeling techniques such as PypeTree [46], TreeQSM [25], and SimpleTree [47]. This method can also control the error between the input point cloud and the final generated model within 10 cm, which provides a significant

advantage in reconstructing complex structural trees in nature. Figure 4 illustrates the complete process of reconstructing a 3D model of a tree based on ALS data, in which Figure 4a represents the initial input point cloud. First, an initial map was constructed by applying a 3D Delaunay triangulation to the input point cloud. An important feature of the Delaunay triangulation is to maximize the minimum diameter of the possible voids in the space. This means that the triangles generated via Delaunay triangulation have the largest possible internal tangent circles, ensuring that there are no large voids, making the topological relationships more accurate. Moreover, the outer circle of each triangle does not contain other points, which guarantees the integrity of the data. At the same time, Delaunay triangulation helps to complete missing regions or incomplete branches. The obtained Delaunay triangular profile is shown in Figure 4b. After obtaining the triangular profile graph, all the edges were weighted according to the length of the edges in the Euclidean space. The shortest paths from all points to the source point (the start of the trunk) were found from the weighted directed graph based on Dijkstra's shortest path algorithm, which serves as the initial skeleton of the tree. Considering that the initial skeleton contains a large number of redundant vertices and edges, the tree skeleton needs to be further simplified. In this work, the simplification was carried out in two main steps: First, weight values were assigned to vertices and edges to remove redundant noise points. Then, the Douglas–Peucker [48] line segment simplification method was employed, and branching simplification was carried out for singleton and multinode nodes by iteratively checking the proximity between neighboring vertices so as to rebuild the lightweight tree skeleton as in Figure 4c. Based on the simplified tree skeleton, the branches were fitted using the cylindrical fitting method, i.e., a 3D tree stereo geometry model with a higher degree of 3D realism was obtained. Compared with the complex curve fitting method, cylindrical fitting is computationally relatively easy and fast. Figure 4d shows the final reconstructed 3D tree skeleton model after cylindrical fitting. Figure 4e demonstrates the degree of alignment of the fitting effect with the original point cloud, in which it can be observed that the point cloud of the original branch is attached to the surface of the fitted branch, while the dense leaf nodes are not involved in the 3D reconstruction process of the branch.

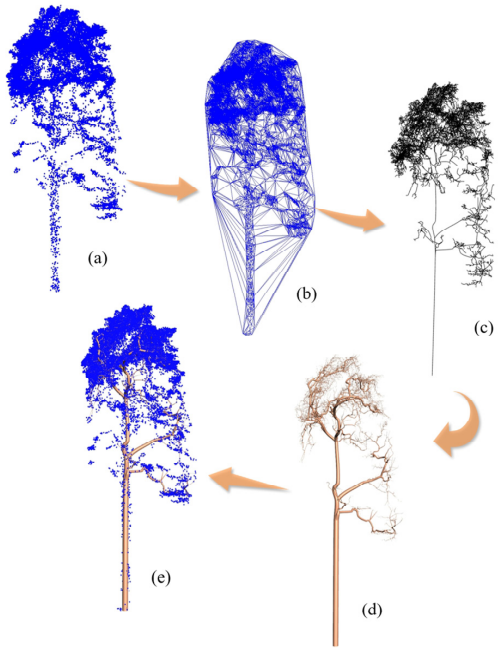

Figure 4. Diagram of the reconstruction process of the camphor pine skeleton based on AdTree. (**a**) Initial input point cloud. (**b**) Delaunay triangular profile. (**c**) lightweight tree skeleton. (**d**) final reconstructed 3D tree skeleton model. (**e**) The degree of alignment with the original point cloud after fitting.

2.5. Model Refinement and Stand Factor Extraction

Currently, the AdTree technique is limited to reconstructing the geometric structure of trees based on scanned point cloud data and has not yet been able to accurately measure the parameters of tree trunks, crowns, and other components. Therefore, the model constructed using this method fails to quantitively assess standing wood factors, and its structural model inherently lacks the ability of quantitative analysis. Based on this, the AdTree algorithm was expanded in this study, and a complete set of stumpage factor estimation methods is proposed to improve the quantitative analysis of stumpage factors. The overall flow chart of the experiment is shown in Figure 5.

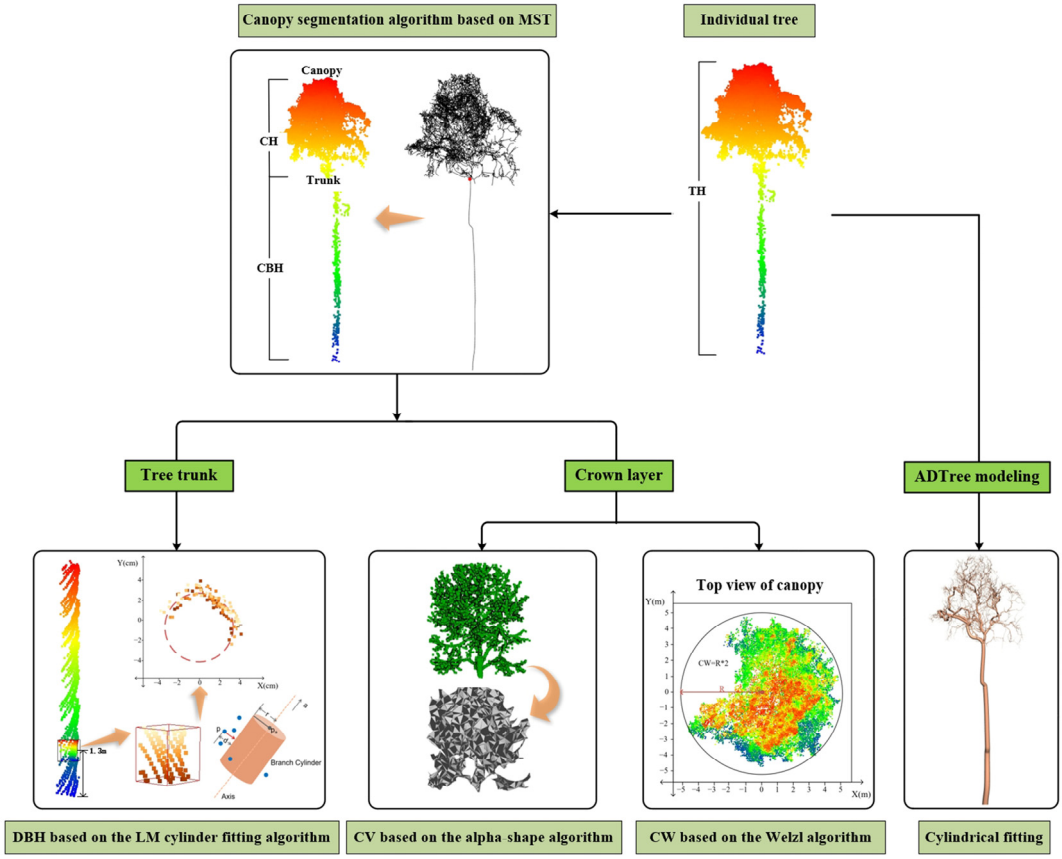

Figure 5. Overall flow chart of the experiment.

1. For tree height (TH) and crown base height (CBH), the maximum and minimum distances from the ground of all crown points on the z-axis of the three-dimensional Cartesian coordinate system were calculated by using connectivity analysis of the detection results;
2. For the value extraction of the diameter at breast height (DBH) feature, a 3D cylinder was fitted to the torso points at the diameter at breast height using the Levenberg–Marquardt-based cylinder fitting algorithm proposed for AdTree;
3. For crown width (CW), a top-down projection was used for the crown points, and the maximum diameter of the crown was retrieved stepwise as the crown diameter using the Welzl algorithm [49];
4. For trunk inclination, the angle between the z-axis and the axis of the fitted cylinder was calculated, which is the tree trunk inclination;
5. For crown volume (CV) characterization, in the methodology of this study, the crown was reconstructed as a watertight enclosing mesh using the crown-point and alpha-shape algorithms, and the estimation of the crown volume was controlled by adjusting the value of the parameter alpha.

This study of model parameter quantification significantly improves the utility of the AdTree reconstruction algorithm, providing not only an accurate reconstruction of tree geometry and topology but also a quantitative analysis of tree parameters within the field of tree modeling and analysis.

2.5.1. Crown Segmentation Method Based on MST Skeleton Map

In the quantitative analysis of the tree, the parameters such as diameter at breast height (DBH), crown base height (CBH), crown width (CW), and crown volume (CV) are based on the information of the main trunk and crown. Therefore, to facilitate the extraction of specific parameters for the crown and trunk, we need to separate the crown and trunk to ensure complete tree point cloud data. Specifically, the method utilizes the AdTree reconstructed tree skeleton map MST to establish the ground contact points of the tree in a 3D spatial Cartesian coordinate system based on the assumption of the minimum z-value attribute. Subsequently, the main axis of the trunk of the tree skeleton map is determined using a graph traversal algorithm by retrieving a path starting from this contact point up the trunk to the bifurcation of the crown and the trunk. In this process, the spatial coordinates of the nodes in the skeleton graph are extracted to form a point set describing the main axis of the trunk. Next, the maximum z-value in the path point set is used as a divider and points smaller than this maximum z-value are filtered out from the complete tree point cloud data as potential trunk point clouds. Finally, a spatial search is performed on these points based on the high-dimensional spatial nearest neighbor search KDTree [50] method to retrieve points neighboring the main axis of the trunk with a certain radius, and these searched points are the original trunk point cloud, which we label as the trunk. Overall, the automatic separation of the trunk from the crown is successfully realized.

2.5.2. Calculating TH and CBH Based on Spatial Connectivity

In a single-tree point cloud, the original point cloud data of the tree need to be downsampled first to reduce the amount of computation and increase the processing rate. The distance between the nearest point clouds in the point cloud downsampling computation must be lower than a predefined threshold to ensure accuracy and to satisfy the requirement of 3D spatial connectivity. Tree height (TH) can be estimated by extracting the maximum and minimum points of the z-axis in 3D Cartesian coordinates from the downsampled individual tree point cloud and calculating the difference between the two z-axes to estimate the tree height (TH). The estimation method of the crown base height (CBH) is the same, and the initial data are the main trunk portion of the tree after the crown is separated from the main trunk. Specifically, the point cloud of the tree trunk after the separation of the crown and the trunk is downsampled, and the difference between the maximum and minimum z-axis points of the downsampled data is extracted to estimate the size of the crown base height (CBH).

2.5.3. DBH Based on LM Cylindrical Fitting Algorithm

Based on the main stem point cloud data, the cylindrical fitting method was used to extract the diameter at breast height (DBH), as this method can effectively avoid the problem of loss of accuracy caused by the fact that the axial and radial directions of the horizontal layer of the main stem point cloud are not calculated together because of the integrated consideration of multidimensional information [26]. In the process of cylindrical fitting, the acquisition of realistic LiDAR data is often accompanied by noise, which is difficult to remove, thus affecting the cylindrical fitting. In order to further improve the accuracy of the extraction results, in this study, we referred to the iterative weighted nonlinear least squares method for AdTree [43], which effectively reduces the impact of noise on the fitting results and improves the stability and accuracy of the fitting. We intercepted the main stem point cloud 1.3 m above and below the ground by expanding the range of 5 cm as the boundary. Cylindrical fitting was performed on the intercepted point cloud segments.

The cylindrical fitting process in three-dimensional space requires the parameters and objective function of the solution, as shown in Figure 6.

- Input data: position p of the input point.
- Parameters to be solved: axial vector a of the cylinder, position p_a of the end point on the axis, and radius r of the cylinder.
- Objective function: the sum of the squares of the distances d from the point to the face of the branching column, with the following formula:

$$\sum_{i=1}^{n} dist(p_i) \quad (1)$$

where dist(p_i) denotes the distance from p_i to the cylinder surface.

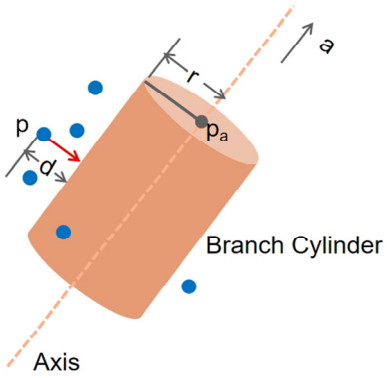

Figure 6. Parameters and objectives of the AdTree-based cylindrical fitting problem.

In order to solve the effect of noise in the process of cylinder fitting, the nonlinear least squares method was adopted based on the Levenberg–Marquardt algorithm [51], which is a commonly used data fitting method that combines the high algorithmic stability of the gradient descent method and the fast convergence of the Gauss–Newton method with their respective advantages. This method can also effectively deal with nonlinear parameter estimation problems. The core idea is to iteratively introduce weighting factors and continuously give different weights to the observations to minimize the residuals between the fitted model and the observed data. The specific idea of weight assignment is based on the distance between the point and the cylinder, giving more weight to points near the cylinder and less weight to points farther away from the cylinder. The weight w_i for a particular point p_i is defined as follows:

$$w_i = 1 - \frac{dist(p_i)}{dist_{max}} \quad (2)$$

where $dist_{max}$ is the maximum distance from all points to the cylinder and dist(p_i) denotes the distance from the current i-th point to the cylinder obtained via initial computation; in this way, we normalized all point weights to the range [0, 1]. The objective function is accordingly expressed as follows:

$$\sum_{i=1}^{n} w_i * dist(p_i) \quad (3)$$

Based on the above objective function, we can fit the segmented cylinder near the breast diameter and solve for the corresponding breast diameter (DBH). Figure 7 shows the intercepted cylinder near the breast diameter with the Levenberg–Marquardt nonlinear least-squares-based fitting process.

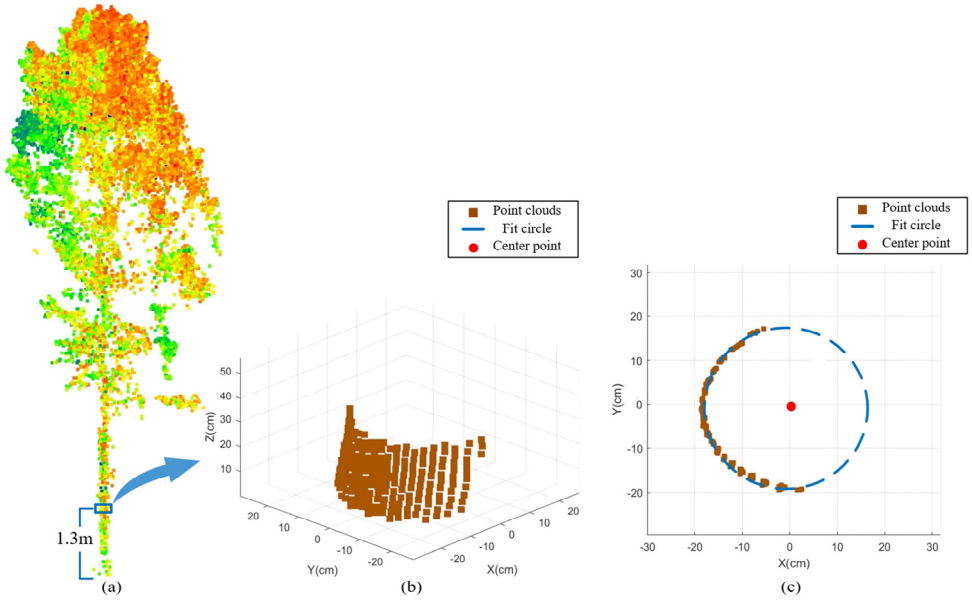

Figure 7. Estimation of DBH based on Levenberg–Marquardt cylindrical fitting algorithm. (**a**) Extract the main stem point cloud within a vertical range around 1.3 m above the ground. (**b**) Side view of the extracted point cloud. (**c**) Top view of the extracted point cloud. The colors of the point clouds in subfigure (**a**) are the "Scalar field" pattern in CloudCompare.

2.5.4. Trunk Lean Angle

Estimating the trunk lean angle is an important step in tree modeling and analysis which helps us to understand tree growth characteristics, structural stability, and evaluation of fall risk, among other aspects. Many of the trees collected in the ALS data have inclined trunks, which are usually not orthogonal to the XY plane.

In studies where trunk angle estimation is performed, it is often necessary to fit three-dimensional cylinders to the trunks in order to more accurately analyze their structural characteristics. In this process, the trunk is decomposed into a series of cylinders, each representing a part of the trunk. By analyzing the position vectors of these decomposed cylinders, important information about the overall shape and inclination of the trunk can be obtained to quantify the spatial orientation of the trunk. Specifically, first, the three-dimensional Cartesian x, y, and z coordinate position vectors of the bottom-most cylinder and the top-most cylinder are determined. These coordinates represent the start- and end-point x, y, and z position vectors of the tree trunk, respectively. By calculating the difference of these two vectors, a new difference vector is obtained, which visually represents the straight-line distance and direction from the bottom to the top of the trunk. Further, the tilt angle of the trunk is obtained by calculating the angle of this resultant vector with respect to the vertical x–y plane. This angle is the degree of deviation of the trunk with respect to the z-axis and is an important parameter for assessing tree growth and structural stability.

2.5.5. Crown Width (CW) Based on Welzl Algorithm

The Welzl [49] algorithm was used in this study to estimate the parameter of crown width. This method demonstrates efficiency and accuracy in calculating crown width values for tree point clouds. Firstly, to process 3D point cloud data, we carried out preprocessing to project the crown point cloud onto a 2D plane to simplify the calculation process. During the projection process, it is crucial to choose the appropriate projection plane and method to ensure that the main features of the data are preserved while minimizing the loss of information. Such preprocessing work lays the foundation for subsequent crown width estimation.

After obtaining the 2D point cloud data, we introduced the Welzl [49] algorithm for processing in order to find the smallest enclosing circle that can completely enclose all the

points. The Welzl [49] algorithm, also known as the smallest enclosing disks algorithm, is an incremental method for calculating the crown width of a vertex given n vertices Sn = {P0, P1, ..., Pn−1} of the smallest enclosing disks. The algorithm is based on the principle that if the point set Si = {P0, P1, ..., Pi−1} of the minimal enclosing sphere is Di, then Di needs to contain another point Pi located outside the sphere Di, and then the new minimal bounding sphere Di + 1 must contain the point Pi on its sphere. A two-dimensional schematic is shown in Figure 8.

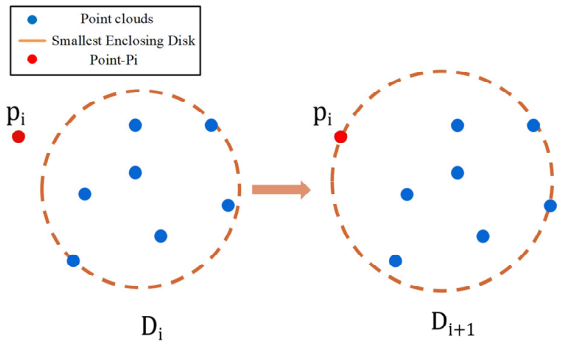

Figure 8. The 2D schematic of the Welzl algorithm.

According to this principle, three points are randomly selected initially to construct a circle, and the center and radius of the circle are dynamically adjusted as points are added one by one until the smallest circle covering all points is found. The top view of the camphor pine canopy is shown in Figure 9. In this process, each time a new point is added, it is checked whether it is within the current circle. If the point is within the current circle, it is not processed; if not, the current circle needs to be extended. The method of extending the circle relies on the processed points and the newly added points to determine the optimal location and size of the new circle by calculating the geometric relationship between them. Eventually, a minimum outer circle containing all the points of the point set is determined using Welzl's algorithm. The diameter of this outer circle is the estimated crown width (CW). To further improve the efficiency of the algorithm and avoid falling into local optimal solutions, we usually randomize the point set before processing. This randomization helps the algorithm to search for the optimal solution globally, rather than relying solely on the order of particular points. Through this process, we are able to estimate the crown width parameter more accurately, which provides reliable data support for subsequent research and applications.

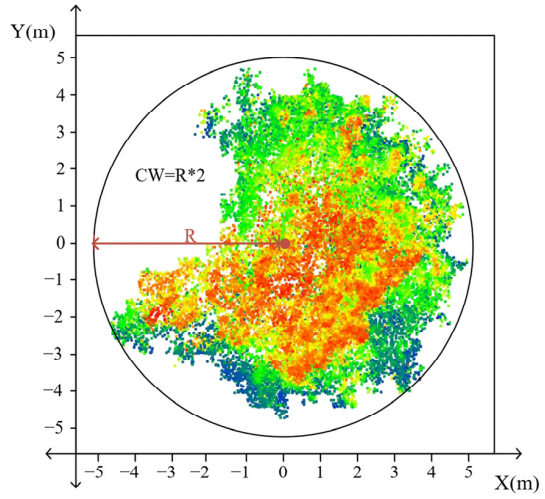

Figure 9. Top view of camphor pine canopy elevation. The colors of the point clouds are the "Scalar field" pattern in CloudCompare.

2.5.6. Alpha-Shape-Based Canopy Volume (CV)

We explored the synthesis and quantification of canopy shapes based on the alpha-shape algorithm for the calculation of the canopy volume (CV) of a canopy point cloud. The alpha-shape algorithm is a geometric reconstruction method based on point cloud data which recovers the geometry of the original dataset by generating a convex polygonal topology and thus restores the geometry of the original dataset. The algorithm adapts to the localized features of the point cloud, generating models that capture voids and concave parts, a property that is particularly important for natural shapes such as tree canopies, which may contain multiple layers and voids. The algorithm was originally proposed in two dimensions and was subsequently extended to three dimensions by Herrero-Huerta et al. [41]. The basic principle is to control the shape of the generated polygons by adjusting the parameter alpha to ensure that the shape is neither overly smooth nor distorted. Figure 10 shows the level of detail in the final canopy corresponding to different alpha values.

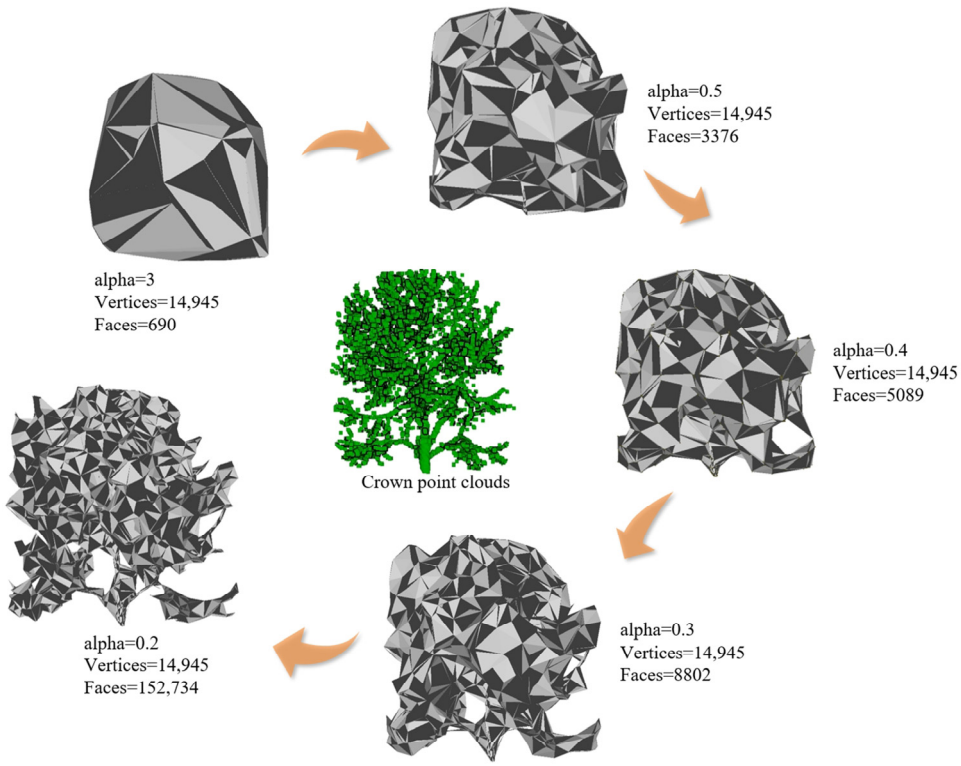

Figure 10. Level of detail in the final canopy corresponding to different alpha values.

The steps of the alpha-shape algorithm include the following:

1. Constructing the Delaunay triangles: the given point cloud data are first subjected to Delaunay triangulation to generate a set of non-overlapping triangular meshes (TINs) covering all data points.
2. Calculating alpha complexes: A crucial part of the alpha-shape algorithm is determining which triangle meshes (TINs) should be included in the alpha complexes. The implementation of this step usually depends on the value of the parameter alpha, which is used to filter the TINs and combine the eligible TINs into alpha complexes. In general, this process is based on the judgment of the radius of the outer circle; if the radius of the outer sphere is less than or equal to alpha, then the corresponding triangles are combined into a set and are known as alpha complexes.
3. Extracting the alpha shape: Edges and vertices are extracted from the alpha complexes, and triangles that are not contained inside any of the external circles are eliminated to form the final alpha shape, which represents the topology of the point cloud data.

4. By adjusting the value of the parameter alpha, geometric reconstruction results with different accuracies and shapes can be obtained. The canopy volume (CV) can be directly estimated based on the final approximated canopy shape.

In the alpha-shape algorithm, the shape of alpha for a finite set of points is a polyhedron uniquely determined using a given set of points and the parameter number alpha [0, ∞]. In the extreme case (alpha = ∞) the shape is close to the convex packet of the given points, and the crown volume (CV) calculated based on this shape may be higher than the true value. As alpha approaches zero, the shape shrinks and gradually forms a cavity, and this overly refined crown shape may result in a lower estimated crown volume than the true value. Therefore, the choice of the alpha value is crucial for the shape of the generated convex polygon in ensuring the accuracy and reliability of the results.

3. Results

In this study, we validated and analyzed the accuracy of the model-extracted parameters such as tree height (TH), crown base height (CBH), diameter at breast height (DBH), crown width (CW), and crown volume (CV) in comparison with the manually measured data. The accuracy of the model was evaluated using the metrics bias, RMSE, R^2, rBias and rRMSE. The corresponding formulas are as follows:

$$Bias = \frac{1}{n}\sum_{i=1}^{n}(y_{pi} - y_i) \tag{4}$$

$$RMSE = \sqrt{\frac{\sum_{i=1}^{n}(y_{pi} - y_i)^2}{n}} \tag{5}$$

$$R^2 = 1 - \frac{\sum_{i=1}^{n}(y_i - y_{pi})^2}{\sum_{i=1}^{n}(y_i - \overline{y_i})^2} \tag{6}$$

$$rBias = \frac{Bias}{\overline{y_i}} \times 100\% \tag{7}$$

$$rRMSE = \frac{RMSE}{\overline{y_i}} \times 100\% \tag{8}$$

In the above equation, i is the current number of samples, n is the total number of samples, y_i is the true value of each sample, y_{pi} is the predicted value of each sample, and $\overline{y_i}$ is the average of the true value of each sample.

We also compared the parameter extraction method in this study with two methods, TreeQSM [25] and AdQSM [26]. The results are shown in Table 2.

Table 2. TH, CBH, DBH, and CW evaluation indexes of the method in this study.

Model	Evaluation Metrics	TH (M)	CBH (M)	DBH (CM)	CW (M)
TreeQSM	Bias	−0.56	−0.58	6.24	0.24
	RMSE	0.81	1.57	10.65	0.95
	R^2	0.73	0.55	0.28	0.50
	rBias	−3.1%	−8.4%	20.3%	4.5%
	rRMSE	4.5%	22.7%	34.6%	17.9%
AdQSM	Bias	−0.30	0.35	9.39	0.60
	RMSE	0.62	1.51	15.44	1.04
	R^2	0.78	0.64	0.09	0.60
	rBias	−1.7%	5.1%	30.5%	11.3%
	rRMSE	3.5%	21.8%	50.1%	19.5%

Table 2. *Cont.*

Model	Evaluation Metrics	TH (M)	CBH (M)	DBH (CM)	CW (M)
Our study	Bias	−0.32	−0.21	0.49	0.03
	RMSE	0.55	1.02	4.10	0.61
	R^2	0.85	0.88	0.63	0.74
	rBias	−1.8%	−3.0%	1.6%	0.6%
	rRMSE	3.1%	14.7%	13.3%	11.5%

3.1. Tree Height and Crown Base Height Results

In the comparative analysis of the model-extracted values with the measured values, it is found that the reference values of field measurements range from 13.8 m to 20.7 m for TH and from 3.4 m to 13.9 m for CBH, whereas in the case of the extracted values based on this paper, the range of the values of TH is from 13.5 m to 19.3 m. The extracted values of CBH are from 2.2 m to 13.4 m. Overall, there is a slight underestimation of the TH and CBH values extracted based on this study compared to the measured values. Specifically, based on the comparison, the model-extracted TH values show a certain degree of negative deviation relative to the measured values. This is confirmed by evaluating the Bias and RMSE of TH. In particular, the Bias value of TH was −0.32 m and the RMSE value was 0.55 m. A total of 92% of the trees had a TH deviation of less than 1 m in absolute value. The Bias value of CBH was −0.21 m and the RMSE value was 1.02 m. Overall, the model-extracted tree heights (TH) and crown base heights (CBH) were basically in agreement with the measured values, which showed a high degree of accuracy. Meanwhile, we compared the two methods of TreeQSM [25] and AdQSM [26]. In terms of TH estimation, the slopes of the corresponding trendline fitting equations of the three methods are all around the number 1, and the corresponding R2 values of this paper and the three methods of TreeQSM [25] and AdQSM [26] are 0.85, 0.73, and 0.77, respectively. In terms of CBH, the R2 values of the scatterplot trendlines of the three methods of this paper and the three methods of TreeQSM [25] and AdQSM [26] were 0.88, 0.55, and 0.64, respectively. The corresponding experimental scatterplots and trend lines for the specific tree height (TH) and crown base height (CBH) are shown in Figure 11.

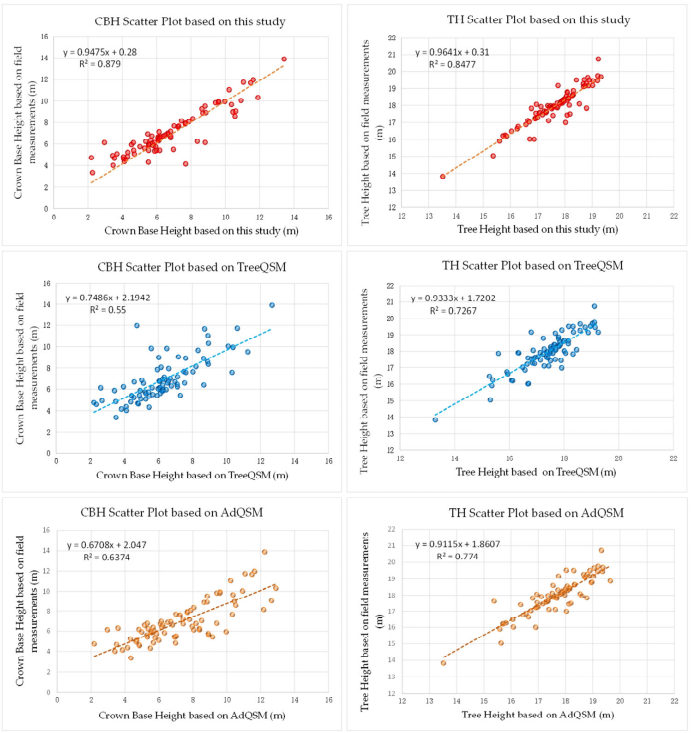

Figure 11. Scatterplots of tree height (TH) and crown base height (CBH).

3.2. Diameter at Breast Height Results

In the collected data, the reference values of the DBH ranged from 14.4 cm to 47.1 cm, and the extracted values based on the method of this study ranged from 19.2 cm to 45.4 cm. The comparative analysis of the DBH measurements showed that the bias of the DBH was 0.49 cm, and the RMSE was 4.1 cm. A total of 89% of the trees in the reference range of 82 camphor pines had a deviation of the DBH of less than 5 cm in absolute terms. The extracted values of breast diameter were evenly distributed on both sides of the reference range. In contrast, the overall breast diameter values estimated based on the TreeQSM [25] and AdQSM [26] methods have a certain degree of positive deviation, and more values are larger than the actual values. The corresponding specific scatter plots and fitted straight lines are shown in Figure 12.

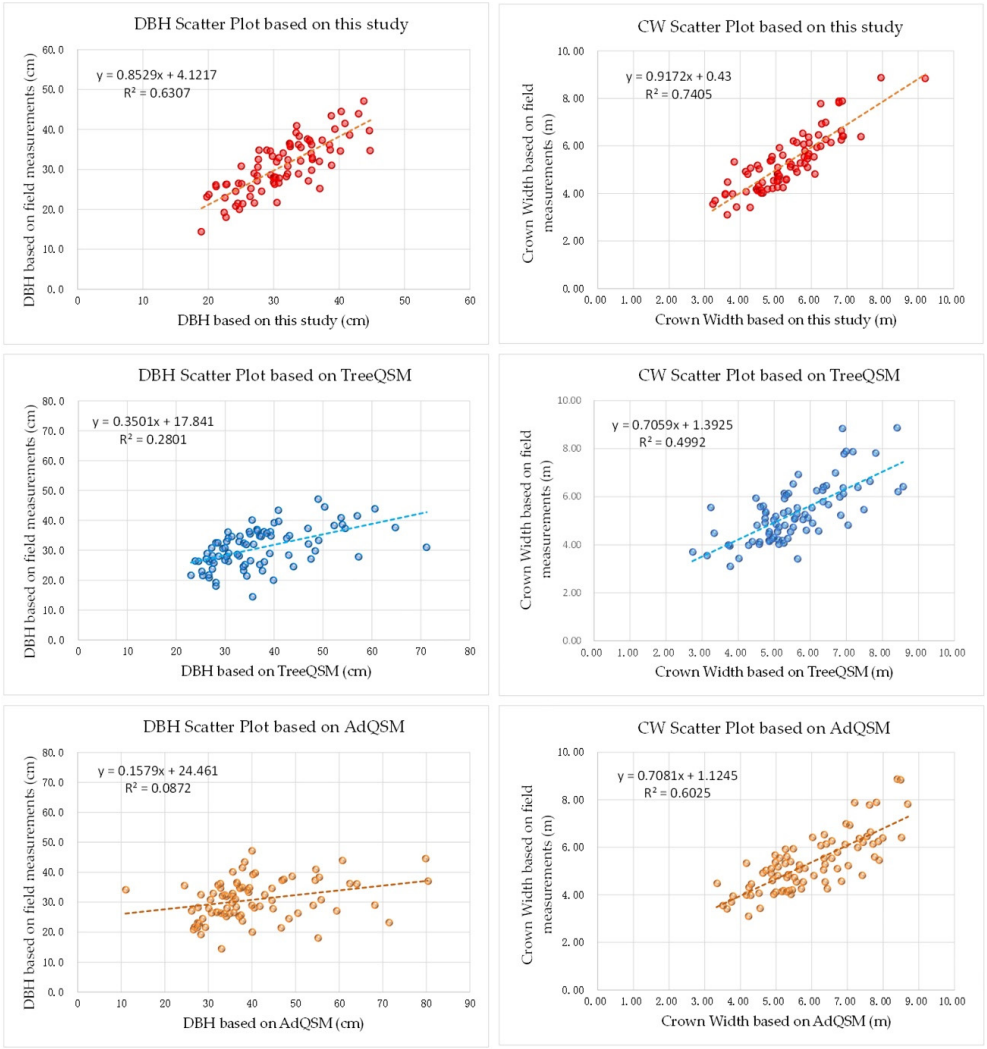

Figure 12. Scatterplots of diameter at breast height (DBH) and crown width (CW).

3.3. Results of Crown Width

The CW of the extracted values based on Welzl's algorithm ranged from 3.22 m to 9.20 m, and the reference values of the field measurements ranged from 3.1 m to 8.87 m. The bias value of the CW was 0.03 m, and the RMSE value was 0.61 m. Nearly 83% of the trees in the experiments had absolute values of CW bias of 0.6 m or less. The scatter plot trend line of the CW had a trend line of R^2 of 0.74, and a slope of 0.9172. Taken together, the high agreement between the algorithmic estimates of CW and the actual measurements demonstrates the effectiveness and stability of this study in capturing CW data.

3.4. Crown Volume Results

As can be seen from Figure 10, the alpha value controls the detail level of the final canopy, and its size selection is especially critical. The selection of an excessive or insufficient alpha value will lead to a canopy value that is too large or small. Take the camphor pine crown in Figure 10 as an example; when alpha = 3, vertices = 14,945, and faces = 690, the crown envelope effect is similar to that of the "convex packet algorithm". The overall shape of the calculated crown volume (CV) is much higher than the real value. When alpha = 0.3, the value of vertices remains unchanged, and the number of faces grows to 8802, which is the closest to the original point cloud and has the best estimation effect. When alpha = 0.2, the number of faces reaches 152,734, indicating over-refinement, and the estimation effect is on the small side. Based on this, we set the overall alpha value to 0.3.

Due to the difficulty of measuring the volume of the tree crown, the most accurate estimation needs to be made by felling the sample trees, and this method cannot protect the tree vegetation in the sampling site. Therefore, the crown volume (CV) extracted based on the TreeQSM [25] algorithm was compared and analyzed with the crown volume (CV) values extracted using the alpha-shape method in this study. The specific data results are shown in Figure 13. The volume extracted based on the alpha algorithm (alpha-shape) in TreeQSM [25] ranges from 2.5 to 126.3 m^3, and the results of these data are closer to the overall results in this study when alpha takes the value of 0.5. In contrast, the crown volume extracted based on the convex hull algorithm in TreeQSM [25] ranges from 22.5 m^3 to 272.5 m^3, showing overall high crown volume values.

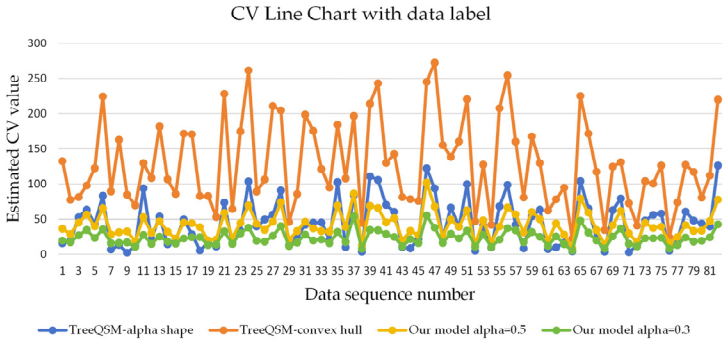

Figure 13. Line plots of crown volume (CV) for different models and parameters.

4. Discussion

4.1. Exploration of Comparisons between Different Models

The aim of this study was to add the quantitative analysis capability of tree attribute estimation to the existing AdTree modeling approach. The quantitative structural modeling of trees based on LiDAR point clouds is still relatively scarce in existing studies. We compared the method of this study with the TreeQSM [25] model and the AdQSM [26] model in terms of the analysis of tree height (TH), crown base height (CBH), diameter at breast height (DBH), crown width (CW), and other parameters for an in-depth analysis of tree attribute estimation.

First, the analysis for the tree height (TH) parameter shows that the slope of the trend line for all three models was close to 1. In the TreeQSM [25] model, we observed that its linear fitting equation was y = 0.9333x + 1.72, with a correlation coefficient (R^2) of 0.73. In the AdQSM [26] model, the slope of the trend line for the tree height was 0.9115, with a correlation coefficient (R^2) of 0.78. These results indicate that both the method proposed in this study and the existing models showed high accuracy and stability in tree height estimation.

Regarding the crown base height (CBH) parameter, the bias and RMSE values of this study and the TreeQSM [25] model were −0.21 m and 1.02 m, and −0.58 m and 1.57 m, respectively, while the bias value of the AdQSM [26] model was 0.35 m, and the RMSE value was 1.51 m. This study's method demonstrated a higher estimation accuracy,

especially in terms of reduced effectiveness in terms of bias. With regard to the scatterplot trendline performance, the overall fitted trendline slope of our study was closer to 1, and the correlation coefficient (R^2) had the largest value, which highlights the superiority of the present study's method in CBH estimation.

In terms of the analysis of diameter at breast height (DBH), this study showed significant advantages over the TreeQSM [25] and AdQSM [26] models. Specifically, the present method demonstrated a lower bias value (0.49 cm), a smaller RMSE (4.1 cm), and a higher correlation coefficient (R^2) (0.63). These indicators reflect the accuracy and reliability of the present method in estimating chest diameter. The other two models, on the other hand, had some degree of positive bias. Specifically, the bias values of TreeQSM [25] and AdQSM [26] were 6.24 cm and 9.39 cm, respectively, and in general, the estimates of the chest diameter using the TreeQSM [25] and AdQSM [26] models were larger than the true values.

In the evaluation index of crown width (CW), the method of this study achieved a greater accuracy advantage, with a trend line slope of 0.9172, and the extracted values of crown width were uniformly distributed on both sides of the reference value. In contrast, the AdQSM [26] and TreeQSM [25] models are less accurate.

In summary, the AdTree modeling technique was thoroughly investigated and optimized in this study through quantitative analysis methods. Significant progress was made, especially in the accuracy and stability of tree attribute estimation. These findings not only enrich the research content in related fields but also provide valuable references and methods for similar work in the future.

4.2. Possible Reasons for the Underestimation of TH and CBH

In the experimental sample of 82 camphor pines, according to the analysis of the obtained data, the bias of the tree height was −0.32 m, and the linear equation of the scatterplot fit was $y = 0.9641x + 0.31$, with a correlation coefficient of $R^2 = 0.85$. The bias of the crown base height was −0.21 m, and the equation of the scatterplot trend line was $y = 0.9475x + 0.28$, with a correlation coefficient of $R^2 = 0.88$. The bias of the tree height was generally similar to the bias of the crown base height. Overall, both the tree height and crown base height values extracted with the model showed a negative deviation relative to the measured values. It was analytically determined that this phenomenon may have originated from the weed layer covering the surface of the study area with a thickness of about 20–35 cm. When employing the CSF-based filtering algorithm, these weeds were misclassified as surface features with a corresponding thickness. As a result, a certain height of the underlying tree trunks may be incorrectly filtered out during the feature separation process, leading to an underestimation of the tree height and crown base height. To address this problem, we need to fully consider and correctly process the height information of the weed layer in the data preprocessing stage to improve the model's accurate measurement of tree dimensions and the accuracy of feature separation.

4.3. Impact of Point Cloud Quality on Parameter Estimation Results

It is important to note that the point cloud quality is directly related to the accuracy and reliability of the resulting parameters and single-tree reconstructions. This uncertainty stems from several factors, including the performance of the laser scanning equipment, environmental conditions, and post-data processing methods. In addition, noise and errors during data processing may further affect the point cloud quality and hence the accuracy of parameter estimation. The influence of point cloud quality on the parameter estimation results is mainly reflected in two aspects: firstly, the influence on the estimation of branch parameters such as breast diameter and height, and secondly, the influence on the modeling effect. The point cloud data based on airborne radar tend to have high-quality canopy information; however, in the highly enclosed camphor pine plantation forest in this experiment, part of the laser could not penetrate the canopy to return branch information. As a result, the density of the collected point clouds in the branch part of the tree was low, and a large number of point clouds of the trunks were missing. From the experimental data,

it can be observed that the bias of the DBH is 0.49 cm, and the RMSE is 4.1 cm. Compared with the canopy parameters, the error is increased to a certain degree. In terms of modeling effect, the single-wood data with varying integrity were compared for the 3D reconstruction experiments, and after comparison, the difference in point cloud quality directly affected the accuracy and reliability of the modeling. As shown in Figure 14, the reconstruction of point clouds with low completeness resulted in lower skeleton realism and completeness. The study by Shenglan Du et al. [11] highlights the importance of point cloud quality on the modeling results.

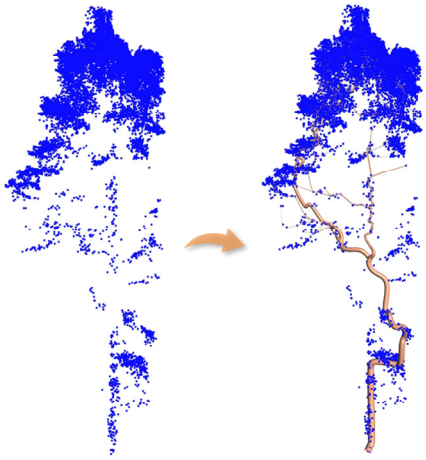

Figure 14. AdTree reconstructions of point clouds with low completeness are also less realistic.

4.4. Limitations of Large-Scale Industry in Terms of Productivity

In large-scale industrial production, enhancing productivity is a critical factor for the widespread application of technological solutions. However, the UAV flight parameters employed in this study—specifically, a flight height of 40 m and a speed of 3 m per second—while appropriate for certain high-precision measurement contexts, significantly restrict the industrial applicability of UAV-based point cloud technology for 3D tree modeling and parameter extraction due to their low productivity. The relatively slow flight speed results in limited area coverage during each flight and prolonged data acquisition times, which are inadequate for the rapid acquisition of high-resolution point cloud data over extensive forested regions. This limitation renders the technology unsuitable for industrial applications that demand efficient data processing, such as large-scale forest monitoring and resource assessment. Consequently, under the current parameter settings, this technology cannot be regarded as a viable solution for large-scale commercial applications.

Nonetheless, this technology retains considerable value in specific scenarios. Theoretically, it can facilitate the establishment of permanent sample plots in remote and challenging terrains for long-term ecological monitoring. Furthermore, the low flight altitude and speed enhance the reliability of high-precision point cloud data acquisition, particularly in complex landscapes or densely vegetated areas. This data can also be utilized to validate forestry taxation assessments, thereby ensuring accuracy and reliability. Overall, while the technology's applicability for large-scale industrial use is limited, it demonstrates significant potential in small-scale, precision-focused applications.

5. Conclusions

Our contribution is to extend the AdTree algorithm by proposing a complete set of stumpage factor estimation methods, which increases the capability of quantitative analysis to obtain stumpage factors by modeling the AdTree method alone. Comprehensive analysis of the above results can lead to the conclusion that the model proposed in this study performs well in the estimation of crown volume (CV), diameter at breast height (DBH), crown width (CW), tree height (TH), and crown base height (CBH), with a certain degree of accuracy and reliability. However, the existence of the height underestimation

phenomenon and the impact of point cloud quality on the accuracy of parameter estimation in this study still need to be noted in practical applications, and it may be necessary to improve the accuracy of the model by further optimizing the data preprocessing steps or increasing the completeness of data collection. Overall, the model in this study has some application prospects in tree structure parameter extraction, especially in the management and monitoring of trees in urban environments and plantation forests with potential value and feasibility. Future research could focus on further optimizing the applicability of the algorithm to different types of trees to improve the prediction accuracy and generalization ability of the model. In addition, enhanced comparative validation with field measurements will help to ensure the reliability and applicability of the model in different scenarios and further promote the development of related fields.

Author Contributions: Methodology, H.W. and D.L.; software, H.W., J.D. and P.S.; investigation, H.W., J.D. and P.S.; writing—original draft preparation, H.W.; writing—review and editing, H.W. and D.L.; format calibration, D.L. All authors have read and agreed to the published version of the manuscript.

Funding: This research received no external funding.

Data Availability Statement: The data sets presented in this article are not readily available due to laboratory policies and confidentiality agreements.

Conflicts of Interest: The authors declare no conflicts of interest.

References

1. Newnham, G.J.; Armston, J.D.; Calders, K.; Disney, M.I.; Lovell, J.L.; Schaaf, C.B.; Strahler, A.H.; Danson, F.M. Terrestrial Laser Scanning for Plot-Scale Forest Measurement. *Curr. For. Rep* **2015**, *1*, 239–251. [CrossRef]
2. Zhou, R.; Sun, H.; Ma, K.; Tang, J.; Chen, S.; Fu, L.; Liu, Q. Improving Estimation of Tree Parameters by Fusing ALS and TLS Point Cloud Data Based on Canopy Gap Shape Feature Points. *Drones* **2023**, *7*, 524. [CrossRef]
3. Zhu, R.; Guo, Z.; Zhang, X. Forest 3D Reconstruction and Individual Tree Parameter Extraction Combining Close-Range Photo Enhancement and Feature Matching. *Remote Sens.* **2021**, *13*, 1633. [CrossRef]
4. Vinci, A.; Brigante, R.; Traini, C.; Farinelli, D. Geometrical Characterization of Hazelnut Trees in an Intensive Orchard by an Unmanned Aerial Vehicle (UAV) for Precision Agriculture Applications. *Remote Sens.* **2023**, *15*, 541. [CrossRef]
5. Holopainen, M.; Vastaranta, M.; Kankare, V.; Hyyppa, H.; Vaaja, M.; Hyyppa, J.; Liang, X.; Litkey, P.; Yu, X.; Kaartinen, H.; et al. The Use of ALS, TLS and VLS Measurements in Mapping and Monitoring Urban Trees. In Proceedings of the 2011 Joint Urban Remote Sensing Event, Munich, Germany, 11–13 April 2011; IEEE: Munich, Germany, 2011; pp. 29–32.
6. Itakura, K.; Miyatani, S.; Hosoi, F. Estimating Tree Structural Parameters via Automatic Tree Segmentation from LiDAR Point Cloud Data. *IEEE J. Sel. Top. Appl. Earth Obs. Remote Sens.* **2022**, *15*, 555–564. [CrossRef]
7. Huang, H.; Li, X.; Chen, C. Individual Tree Crown Detection and Delineation From Very-High-Resolution UAV Images Based on Bias Field and Marker-Controlled Watershed Segmentation Algorithms. *IEEE J. Sel. Top. Appl. Earth Obs. Remote Sens.* **2018**, *11*, 2253–2262. [CrossRef]
8. Zhou, R.; Wu, D.; Zhou, R.; Fang, L.; Zheng, X.; Lou, X. Estimation of DBH at Forest Stand Level Based on Multi-Parameters and Generalized Regression Neural Network. *Forests* **2019**, *10*, 778. [CrossRef]
9. Brovkina, O.; Latypov, I.S.; Cienciala, E.; Fabianek, T. Improved Method for Estimating Tree Crown Diameter Using High-Resolution Airborne Data. *JARS* **2016**, *10*, 026006. [CrossRef]
10. Kurdi, F.T.; Lewandowicz, E.; Shan, J.; Gharineiat, Z. Three-Dimensional Modeling and Visualization of Single Tree LiDAR Point Cloud Using Matrixial Form. *IEEE J. Sel. Top. Appl. Earth Obs. Remote Sens.* **2024**, *17*, 3010–3022. [CrossRef]
11. Du, S.; Lindenbergh, R.; Ledoux, H.; Stoter, J.; Nan, L. AdTree: Accurate, Detailed, and Automatic Modelling of Laser-Scanned Trees. *Remote Sens.* **2019**, *11*, 2074. [CrossRef]
12. Honda, H. Description of the Form of Trees by the Parameters of the Tree-like Body: Effects of the Branching Angle and the Branch Length on the Shape of the Tree-like Body. *J. Theor. Biol.* **1971**, *31*, 331–338. [CrossRef] [PubMed]
13. Okabe, M.; Owada, S.; Igarashi, T. Interactive Design of Botanical Trees Using Freehand Sketches and Example-Based Editing. In Proceedings of the ACM SIGGRAPH 2007 Courses, San Diego, CA, USA, 5–9 August 2007; ACM: San Diego, CA, USA, 2007; p. 26.
14. Li, B.; Kałużny, J.; Klein, J.; Michels, D.L.; Pałubicki, W.; Benes, B.; Pirk, S. Learning to Reconstruct Botanical Trees from Single Images. *ACM Trans. Graph.* **2021**, *40*, 1–15. [CrossRef]
15. Livny, Y.; Yan, F.; Olson, M.; Chen, B.; Zhang, H.; El-Sana, J. Automatic Reconstruction of Tree Skeletal Structures from Point Clouds. *ACM Trans. Graph.* **2010**, *29*, 151. [CrossRef]
16. Wang, W.; Li, Y.; Huang, H.; Hong, L.; Du, S.; Xie, L.; Li, X.; Guo, R.; Tang, S. Branching the Limits: Robust 3D Tree Reconstruction from Incomplete Laser Point Clouds. *Int. J. Appl. Earth Obs. Geoinf.* **2023**, *125*, 103557. [CrossRef]

17. Liang, X.; Kukko, A.; Kaartinen, H.; Hyyppä, J.; Yu, X.; Jaakkola, A.; Wang, Y. Possibilities of a Personal Laser Scanning System for Forest Mapping and Ecosystem Services. *Sensors* **2014**, *14*, 1228–1248. [CrossRef]
18. González-Jorge, H.; Rodríguez-Gonzálvez, P.; Shen, Y.; Lagüela, S.; Díaz-Vilariño, L.; Lindenbergh, R.; González-Aguilera, D.; Arias, P. Metrological Intercomparison of Six Terrestrial Laser Scanning Systems. *IET Sci. Meas. Technol.* **2018**, *12*, 218–222. [CrossRef]
19. Kuželka, K.; Slavík, M.; Surový, P. Very High Density Point Clouds from UAV Laser Scanning for Automatic Tree Stem Detection and Direct Diameter Measurement. *Remote Sens.* **2020**, *12*, 1236. [CrossRef]
20. Seidel, D.; Ehbrecht, M.; Annighöfer, P.; Ammer, C. From Tree to Stand-Level Structural Complexity—Which Properties Make a Forest Stand Complex? *Agric. For. Meteorol.* **2019**, *278*, 107699. [CrossRef]
21. Qi, W.; Dubayah, R.O. Combining Tandem-X InSAR and Simulated GEDI Lidar Observations for Forest Structure Mapping. *Remote Sens. Environ.* **2016**, *187*, 253–266. [CrossRef]
22. Estornell, J.; Hadas, E.; Martí, J.; López-Cortés, I. Tree Extraction and Estimation of Walnut Structure Parameters Using Airborne LiDAR Data. *Int. J. Appl. Earth Obs. Geoinf.* **2021**, *96*, 102273. [CrossRef]
23. Holopainen, M.; Kankare, V.; Vastaranta, M.; Liang, X.; Lin, Y.; Vaaja, M.; Yu, X.; Hyyppä, J.; Hyyppä, H.; Kaartinen, H.; et al. Tree Mapping Using Airborne, Terrestrial and Mobile Laser Scanning—A Case Study in a Heterogeneous Urban Forest. *Urban For. Urban Green.* **2013**, *12*, 546–553. [CrossRef]
24. Sun, P.; Yuan, X.; Li, D. Classification of Individual Tree Species Using UAV LiDAR Based on Transformer. *Forests* **2023**, *14*, 484. [CrossRef]
25. Raumonen, P.; Kaasalainen, M.; Åkerblom, M.; Kaasalainen, S.; Kaartinen, H.; Vastaranta, M.; Holopainen, M.; Disney, M.; Lewis, P. Fast Automatic Precision Tree Models from Terrestrial Laser Scanner Data. *Remote Sens.* **2013**, *5*, 491–520. [CrossRef]
26. Fan, G.; Nan, L.; Dong, Y.; Su, X.; Chen, F. AdQSM: A New Method for Estimating Above-Ground Biomass from TLS Point Clouds. *Remote Sens.* **2020**, *12*, 3089. [CrossRef]
27. Calders, K.; Newnham, G.; Burt, A.; Murphy, S.; Raumonen, P.; Herold, M.; Culvenor, D.; Avitabile, V.; Disney, M.; Armston, J.; et al. Nondestructive Estimates of Above-Ground Biomass Using Terrestrial Laser Scanning. *Methods Ecol. Evol.* **2015**, *6*, 198–208. [CrossRef]
28. Trochta, J.; Krůček, M.; Vrška, T.; Král, K. 3D Forest: An Application for Descriptions of Three-Dimensional Forest Structures Using Terrestrial LiDAR. *PLoS ONE* **2017**, *12*, e0176871. [CrossRef]
29. Zhou, S.; Kang, F.; Li, W.; Kan, J.; Zheng, Y.; He, G. Extracting Diameter at Breast Height with a Handheld Mobile LiDAR System in an Outdoor Environment. *Sensors* **2019**, *19*, 3212. [CrossRef]
30. Olofsson, K.; Holmgren, J.; Olsson, H. Tree Stem and Height Measurements Using Terrestrial Laser Scanning and the RANSAC Algorithm. *Remote Sens.* **2014**, *6*, 4323–4344. [CrossRef]
31. Yang, B.; Dai, W.; Dong, Z.; Liu, Y. Automatic Forest Mapping at Individual Tree Levels from Terrestrial Laser Scanning Point Clouds with a Hierarchical Minimum Cut Method. *Remote Sens.* **2016**, *8*, 372. [CrossRef]
32. Yubo, L.; Hongyu, H.; Liyu, T.; Chongcheng, C.; Hao, Z. Tree Height and Diameter Extraction with 3D Reconstruction in a Forest Based on TLS. *Remote Sens. Technol. Appl.* **2019**, *34*, 243–252.
33. Dai, M.; Li, G. Soft Segmentation and Reconstruction of Tree Crown from Laser Scanning Data. *Electronics* **2023**, *12*, 2300. [CrossRef]
34. Rautiainen, M.; Mõttus, M.; Stenberg, P.; Ervasti, S. Crown Envelope Shape Measurements and Models. *Silva Fenn.* **2008**, *42*, 261. [CrossRef]
35. Franceschi, E.; Moser-Reischl, A.; Rahman, M.A.; Pauleit, S.; Pretzsch, H.; Rötzer, T. Crown Shapes of Urban Trees-Their Dependences on Tree Species, Tree Age and Local Environment, and Effects on Ecosystem Services. *Forests* **2022**, *13*, 748. [CrossRef]
36. Chen, X.; Jiang, K.; Zhu, Y.; Wang, X.; Yun, T. Individual Tree Crown Segmentation Directly from UAV-Borne LiDAR Data Using the PointNet of Deep Learning. *Forests* **2021**, *12*, 131. [CrossRef]
37. Cluzeau, C.; Dupouey, J.; Courbaud, B. Polyhedral Representation of Crown Shape. A Geometric Tool for Growth Modelling. *Ann. For. Sci.* **1995**, *52*, 297–306. [CrossRef]
38. Lin, W.; Meng, Y.; Qiu, Z.; Zhang, S.; Wu, J. Measurement and Calculation of Crown Projection Area and Crown Volume of Individual Trees Based on 3D Laser-Scanned Point-Cloud Data. *Int. J. Remote Sens.* **2017**, *38*, 1083–1100. [CrossRef]
39. Zhu, Z.; Kleinn, C.; Nölke, N. Assessing Tree Crown Volume—A Review. *For. Int. J. For. Res.* **2021**, *94*, 18–35. [CrossRef]
40. Phattaralerphong, J.; Sinoquet, H. A Method for 3D Reconstruction of Tree Crown Volume from Photographs: Assessment with 3D-Digitized Plants. *Tree Physiol.* **2005**, *25*, 1229–1242. [CrossRef] [PubMed]
41. Lecigne, B.; Delagrange, S.; Messier, C. Exploring Trees in Three Dimensions: VoxR, a Novel Voxel-Based R Package Dedicated to Analysing the Complex Arrangement of Tree Crowns. *Ann. Bot.* **2018**, *121*, 589–601. [CrossRef]
42. Zhu, C.; Zhang, X.; Hu, B.; Jaeger, M. Reconstruction of Tree Crown Shape from Scanned Data. In *Technologies for E-Learning and Digital Entertainment*; Pan, Z., Zhang, X., El Rhalibi, A., Woo, W., Li, Y., Eds.; Lecture Notes in Computer Science; Springer: Berlin/Heidelberg, Germany, 2008; Volume 5093, pp. 745–756; ISBN 978-3-540-69734-3.
43. Herrero-Huerta, M.; Lindenbergh, R.; Rodríguez-Gonzálvez, P. Automatic Tree Parameter Extraction by a Mobile LiDAR System in an Urban Context. *PLoS ONE* **2018**, *13*, e0196004. [CrossRef]

44. Zhang, W.; Qi, J.; Wan, P.; Wang, H.; Xie, D.; Wang, X.; Yan, G. An Easy-to-Use Airborne LiDAR Data Filtering Method Based on Cloth Simulation. *Remote Sens.* **2016**, *8*, 501. [CrossRef]
45. Shendryk, I.; Broich, M.; Tulbure, M.G.; Alexandrov, S.V. Bottom-up Delineation of Individual Trees from Full-Waveform Airborne Laser Scans in a Structurally Complex Eucalypt Forest. *Remote Sens. Environ.* **2016**, *173*, 69–83. [CrossRef]
46. Delagrange, S.; Jauvin, C.; Rochon, P. PypeTree: A Tool for Reconstructing Tree Perennial Tissues from Point Clouds. *Sensors* **2014**, *14*, 4271–4289. [CrossRef] [PubMed]
47. Hackenberg, J.; Spiecker, H.; Calders, K.; Disney, M.; Raumonen, P. SimpleTree—An Efficient Open Source Tool to Build Tree Models from TLS Clouds. *Forests* **2015**, *6*, 4245–4294. [CrossRef]
48. Wu, S.-T.; Marquez, M.R.G. A Non-Self-Intersection Douglas-Peucker Algorithm. In Proceedings of the 16th Brazilian Symposium on Computer Graphics and Image Processing (SIBGRAPI 2003), Sao Carlos, Brazil, 12–15 October 2003; IEEE Computer Society: Sao Carlos, Brazil, 2003; pp. 60–66.
49. Welzl, E. Smallest Enclosing Disks (Balls and Ellipsoids). In *New Results and New Trends in Computer Science*; Maurer, H., Ed.; Lecture Notes in Computer Science; Springer: Berlin/Heidelberg, Germany, 1991; Volume 555, pp. 359–370; ISBN 978-3-540-54869-0.
50. Muja, M.; Lowe, D.G. Scalable Nearest Neighbor Algorithms for High Dimensional Data. *IEEE Trans. Pattern Anal. Mach. Intell.* **2014**, *36*, 2227–2240. [CrossRef]
51. Levenberg, K. A Method for the Solution of Certain Non-Linear Problems in Least Squares. *Quart. Appl. Math.* **1944**, *2*, 164–168. [CrossRef]